Supplementary Information (SI) for Journal of Materials Chemistry C.

Supplementary materials

Shape Customization of 2D Materials by Maskless Ultrafast Laser Lithography

*Weiqing Wu[1], Luchan Lin[1] *, Xiaoyang Fu[2], Yifan Hu[1], Junde Ji[1], Xinde Zuo[1], Yiwei Yu[1], and Zhuguo Li[1] **

[1]Shanghai Key Laboratory of Materials Laser Processing and Modification, School of Materials Science and Engineering, Shanghai Jiao Tong University, Shanghai 200240, China.

[2]School of Materials Science and Engineering, Peking University, Beijing, 100871, China

E-mail: luchan.lin@sjtu.edu.cn; lizg@sjtu.edu.cn.

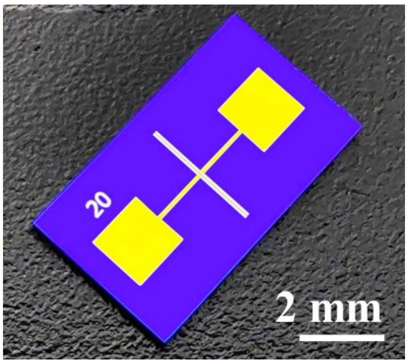

Fig. S1 Photograph of parallel electrodes

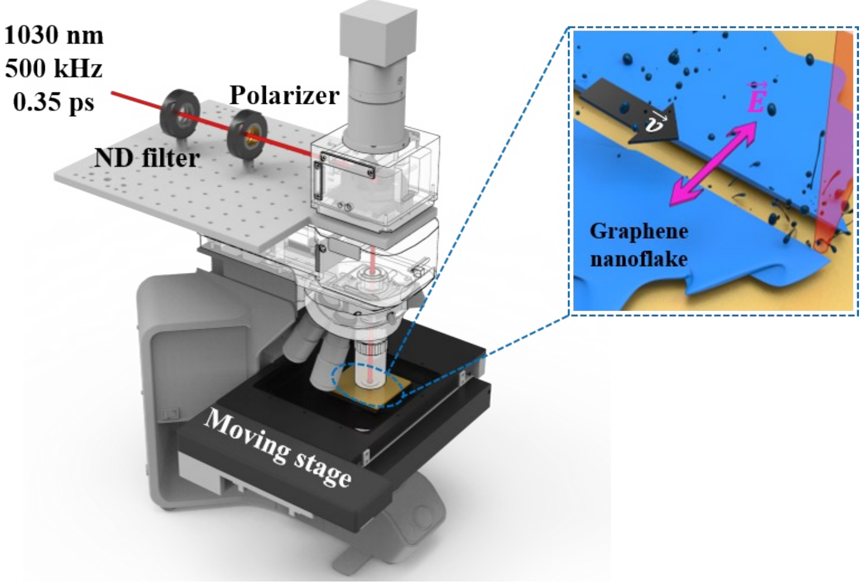

Fig. S2 Experimental setup for ultrafast laser lithography.

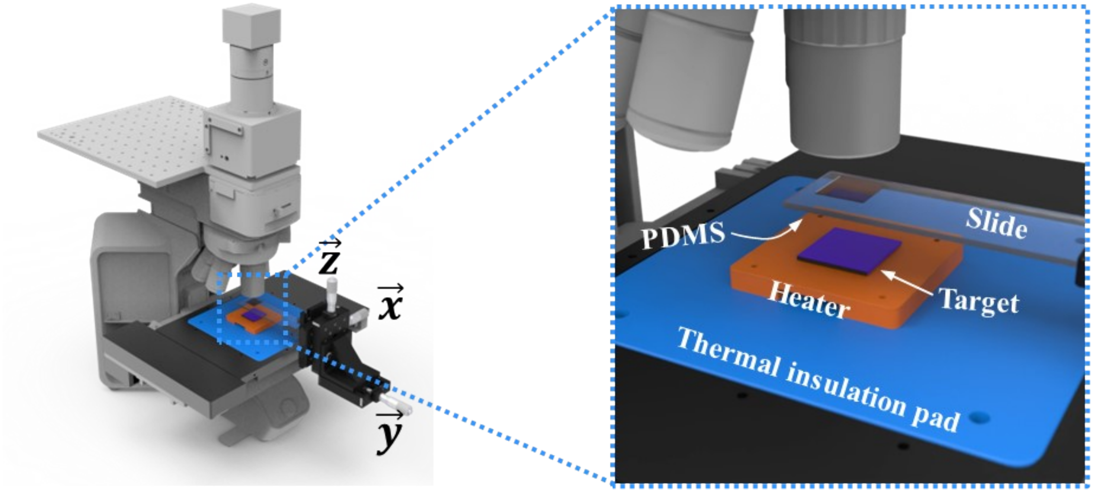

Fig. S3 Schematic of the PDMS-based dry transfer process for nanoflakes.

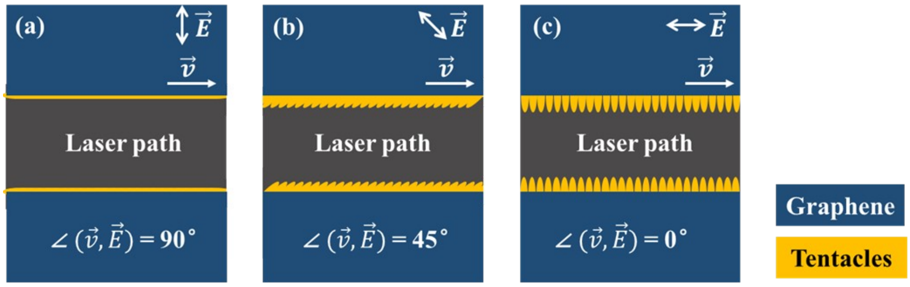

Fig. S4 Illustration of the tentacle-like structure orientation under laser scanning with different angles. (a) Polarization ⊥ scanning. (b) Angled 45°. (c) Polarization ∥ scanning.

The angle between laser polarization direction and scanning path directly influences edge smoothness:

(1) Polarization ⊥ scanning: Tentacle-shaped structures align parallel to the ablation edge, and smooth ablation edges have been achieved (Fig. S4a).

(2) Angled 45°: The tilted tentacle-shaped structures start to appear along the ablation edge, which is the result of the periodic redistributed laser energy (Fig. S4b).

(3) Polarization ∥ scanning: Tentacle-shaped structures become perpendicular to the edge to create deep grooves that increases the roughness greatly (Fig. S4c).

Therefore, as the angle between the polarization direction and scanning direction increases (up to 90°), the roughness of ablated edges decreases accordingly.

Related discussion has been added in the revised manuscript.

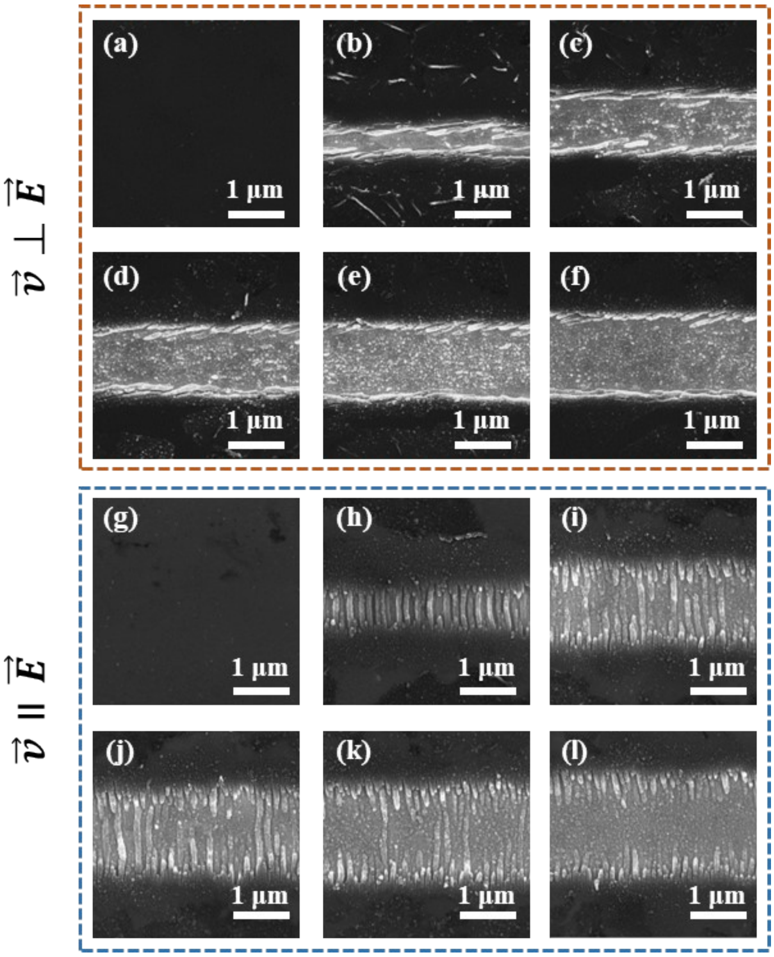

Fig. S5 SEM images of ultrafast laser ablated graphene nanoflakes on gold at different laser fluences and polarization directions. Laser polarization was perpendicular to the scanning direction with laser fluence of (a) 0.69 J cm^{-2}, (b) 0.87 J cm^{-2}, (c) 1.04 J cm^{-2}, (d) 1.21 J cm^{-2}, (e) 1.39 J cm^{-2}, (f) 1.56 J cm^{-2}. Laser polarization was parallel to the scanning direction with laser fluence of (g) 0.69 J cm^{-2}, (h) 0.87 J cm^{-2}, (i) 1.04 J cm^{-2}, (j) 1.21 J cm^{-2}, (k) 1.39 J cm^{-2} and (l) 1.56 J cm^{-2}. Substrate: gold coated silicon wafer. Pulse duration: 350 fs. Scanning speed: 10 μm/s. Repetition rate: 800 kHz.

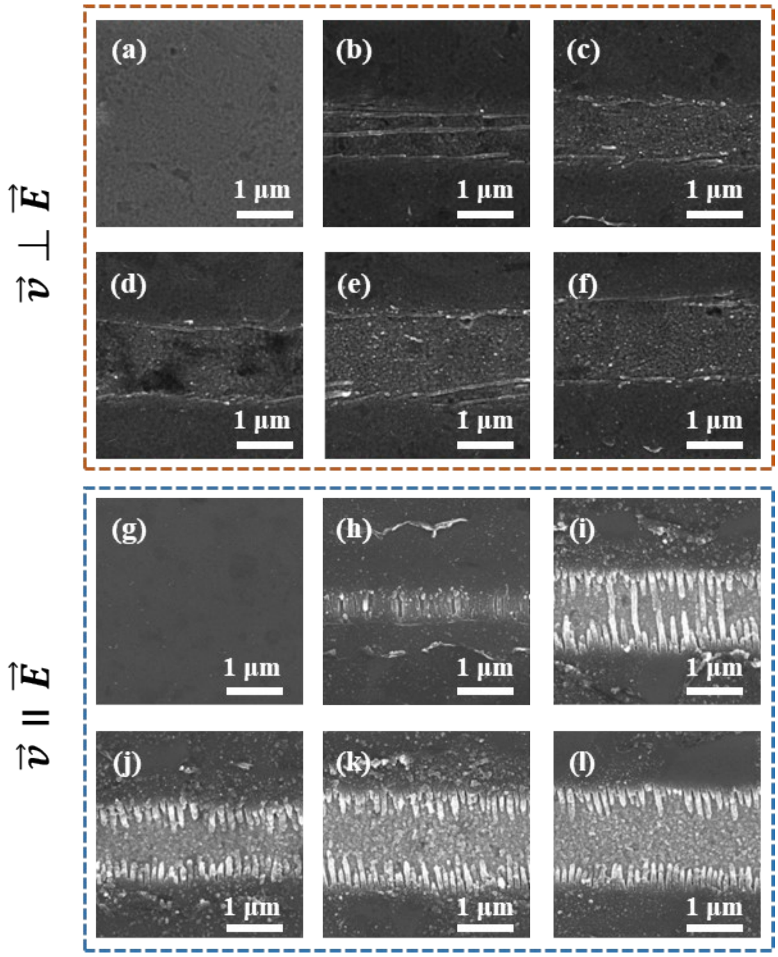

Fig. S6 SEM images of ultrafast laser ablated graphene nanoflakes on copper at different laser fluences and polarization directions. Laser polarization was perpendicular to the scanning direction with laser fluence of (a) 0.69 J cm^{-2}, (b) 0.87 J cm^{-2}, (c) 1.04 J cm^{-2}, (d) 1.21 J cm^{-2}, (e) 1.39 J cm^{-2}, (f) 1.56 J cm^{-2}. Laser polarization was parallel to the scanning direction with laser fluence of (g) 0.69 J cm^{-2}, (h) 0.87 J cm^{-2}, (i) 1.04 J cm^{-2}, (j) 1.21 J cm^{-2}, (k) 1.39 J cm^{-2} and (l) 1.56 J cm^{-2}. Substrate: copper coated silicon wafer. Pulse duration: 350 fs. Scanning speed: 10 µm/s. Repetition rate 800: kHz.

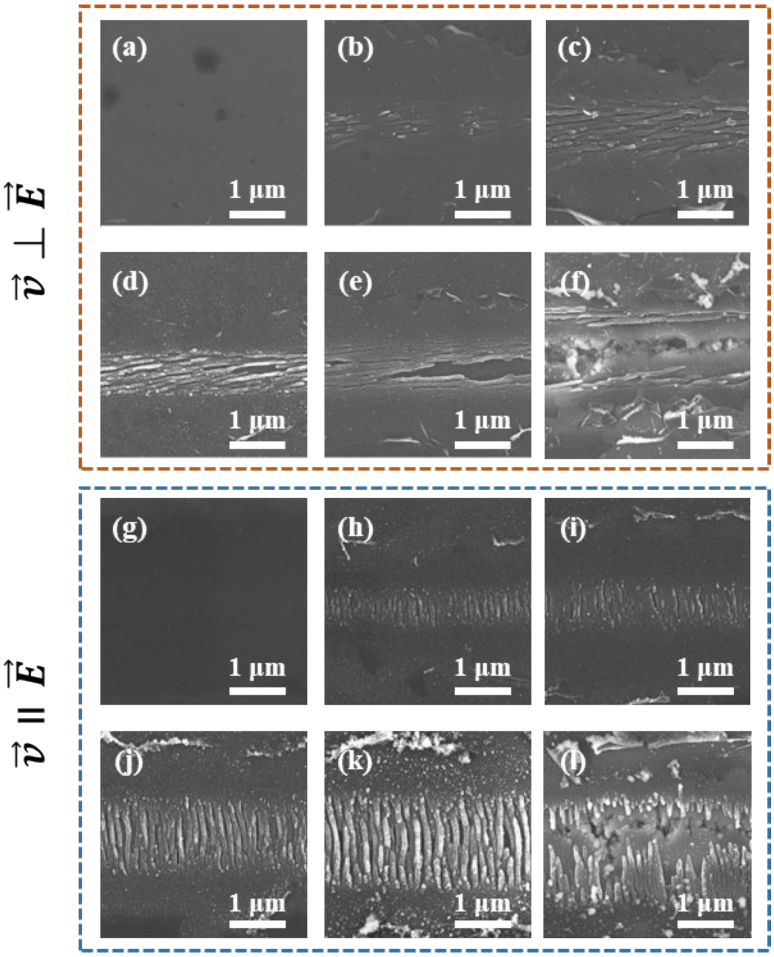

Fig. S7 SEM images of ultrafast laser ablated graphene nanoflakes on silica at different laser fluences and polarization directions. Laser polarization was perpendicular to the scanning direction with laser fluence of (a) 1.21 J cm^{-2}, (b) 1.39 J cm^{-2}, (c) 1.56 J cm^{-2}, (d) 1.73 J cm^{-2}, (e) 1.91 J cm^{-2}, (f) 2.08 J cm^{-2}. Laser polarization was parallel to the scanning direction with laser fluence of (g) 1.21 J cm^{-2}, (h) 1.39 J cm^{-2}, (i) 1.56 J cm^{-2}, (j) 1.73 J cm^{-2}, (k) 1.91 J cm^{-2} and (l) 2.08 J cm^{-2}. Substrate: silica coated silicon wafer. Pulse duration: 350 fs. Scanning speed: 10 μm/s. Repetition rate: 800 kHz.

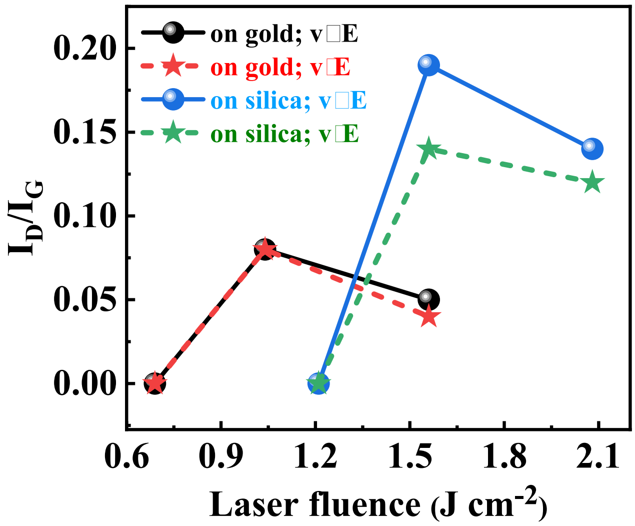

Fig. S8 I_D/I_G as a function of incident laser energy for samples being irradiated on gold-coated and silica-coated substrate.

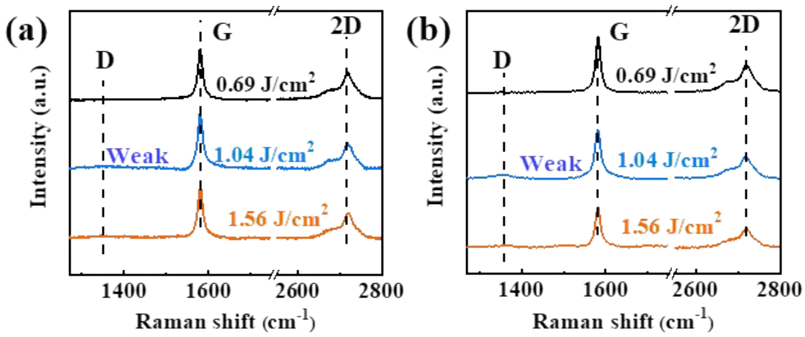

Fig. S9 Raman spectra of ultrafast laser ablated graphene nanoflakes on copper at different laser fluences: (a) Laser polarization was perpendicular to the scanning direction, (b) Laser polarization was parallel to the scanning direction.

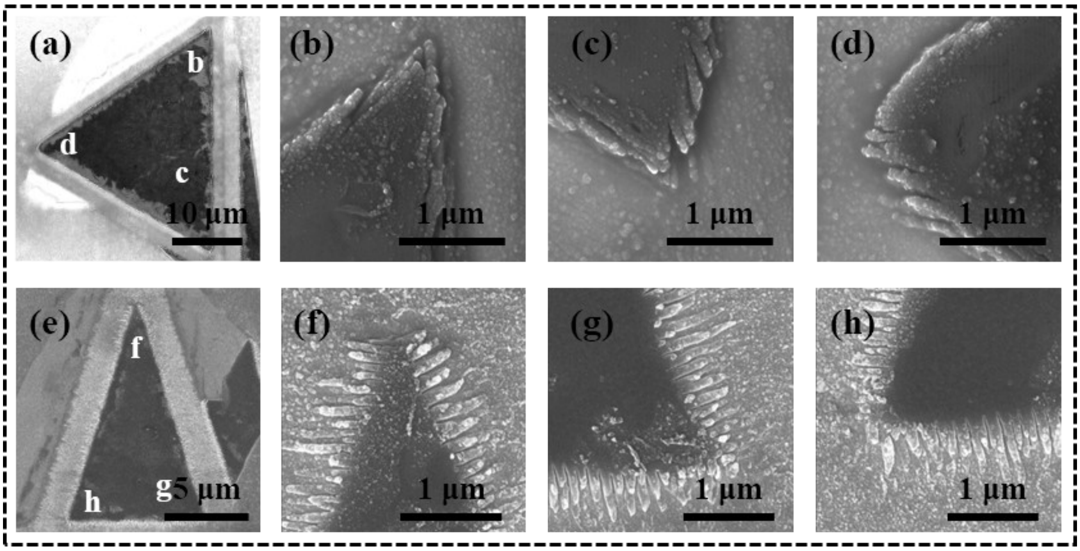

Fig. S10 (a) SEM image of triangular graphene nanoflake with smooth edges after ultrafast laser lithography. (b-d) Magnified SEM images of laser ablated corners in (a). Laser polarization was always perpendicular to the scanning direction during ultrafast laser ablation in (a). (e) SEM image of triangular graphene nanoflake with rough edges after ultrafast laser lithography. (f-h) Magnified SEM images of laser ablated corners in (e). Laser polarization was always parallel to the scanning direction during ultrafast laser ablation in (e). Laser fluence: 1.56 J cm^{-2}. Pulse duration: 350 fs. Scanning speed: 10 μm/s. Repetition rate: 800 kHz.

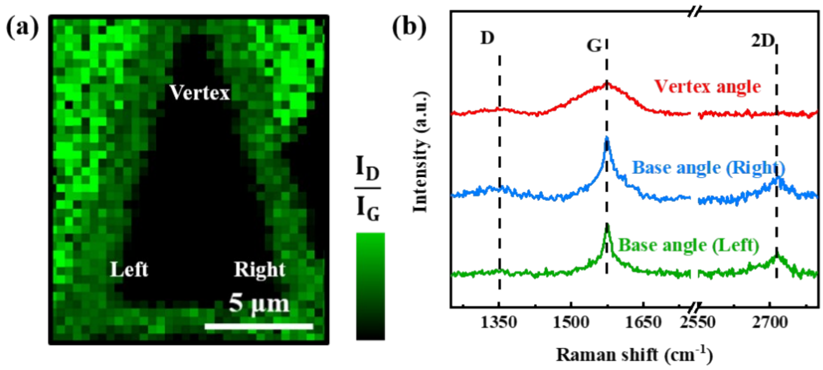

Fig. S11 (a) Raman mapping of triangular graphene nanoflake with rough edges in **Fig. S9**e. The intensity of color bar represents the ratio of I_D and I_G. (b) Raman spectra measured at the laser ablated corners of the triangle graphene nanoflake.

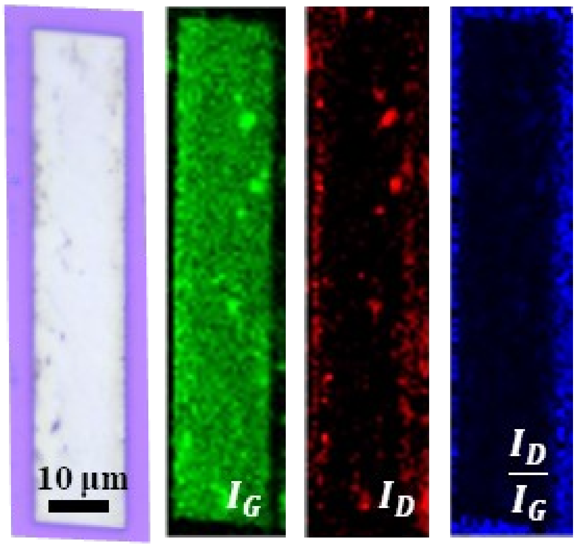

Fig. S12 Optical image and Raman mapping of ultrafast laser tailored parallelogram graphene nanoflake. Laser fluence: 1.56 J cm^{-2}. Pulse duration: 350 fs. Scanning speed: 10 µm/s. Repetition rate: 800 kHz.

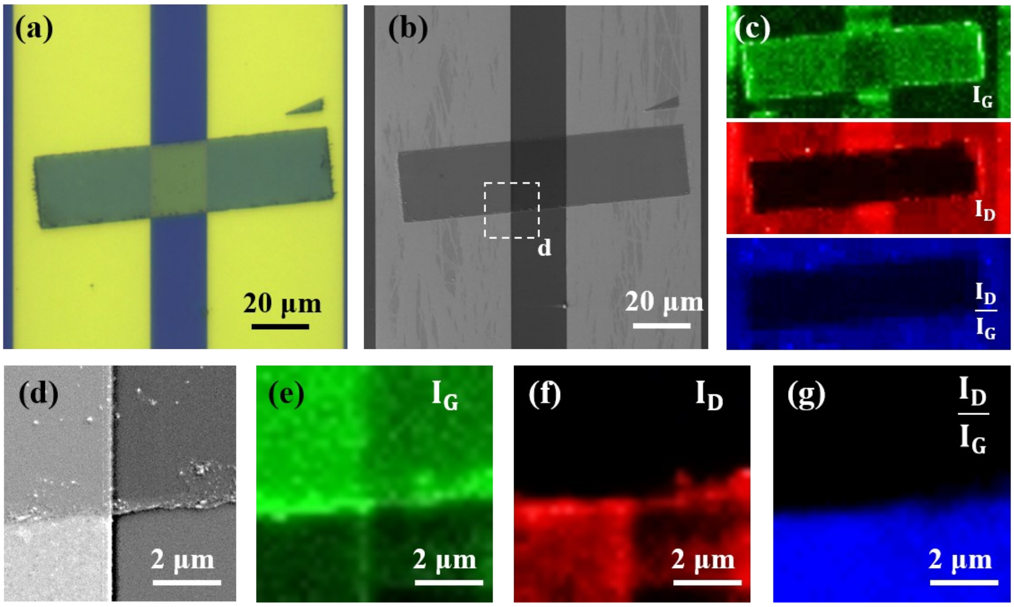

Fig. S13 (a) Optical image of the nanocircuit composed of an ultrafast laser tailored rectangular-shaped graphene nanoflake. (b) Corresponding SEM image of the nanocircuit in (a). (c) Raman mapping of ultrafast laser tailored rectangular-shaped graphene nanoflake with the typical G peak, D peak, and the Raman peak intensity ratio of D peak and G peak. (d) SEM image and (e-g) Raman intensity mapping of G-band peak, D-band peak and the ratio of D peak and G peak at the contact area between graphene nanoflake and metal electrode.

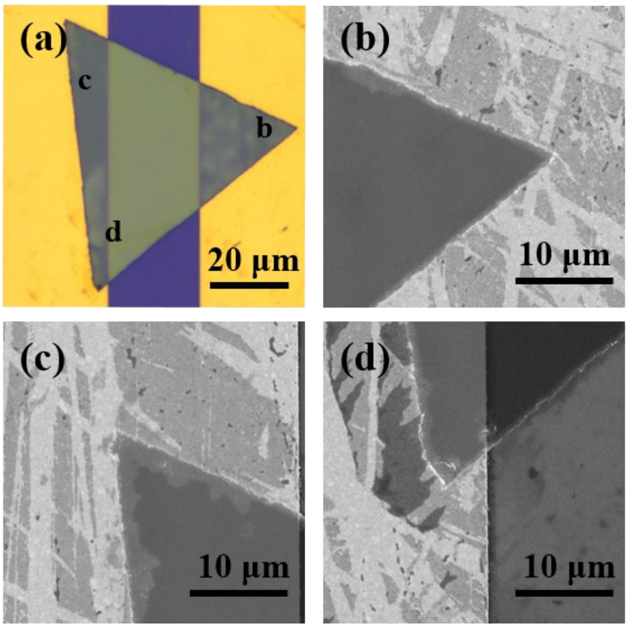

Fig. S14 (a) Optical image of the nanocircuit composed of an ultrafast laser tailored triangle-shaped graphene nanoflake. (b-d) SEM images of ultrafast laser tailored corners of the triangular graphene nanoflake.

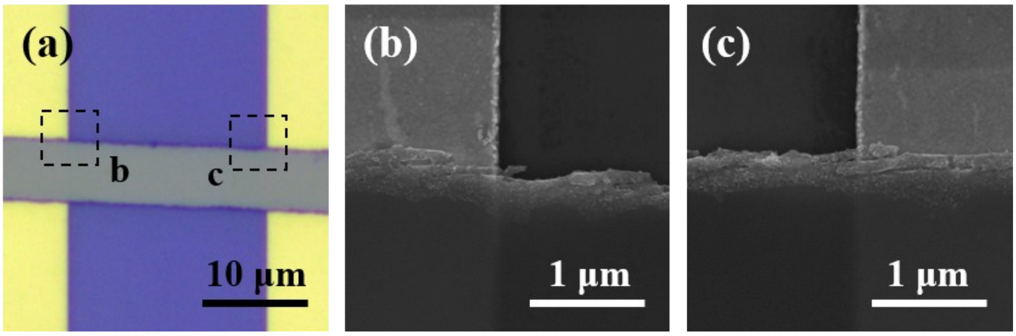

Fig. S15 (a) Optical image of the nanocircuit composed of an ultrafast laser tailored ultra-narrow rectangular-shaped graphene nanoflake. (b-c) SEM images of the contacts between graphene and electrode indicated in (a).

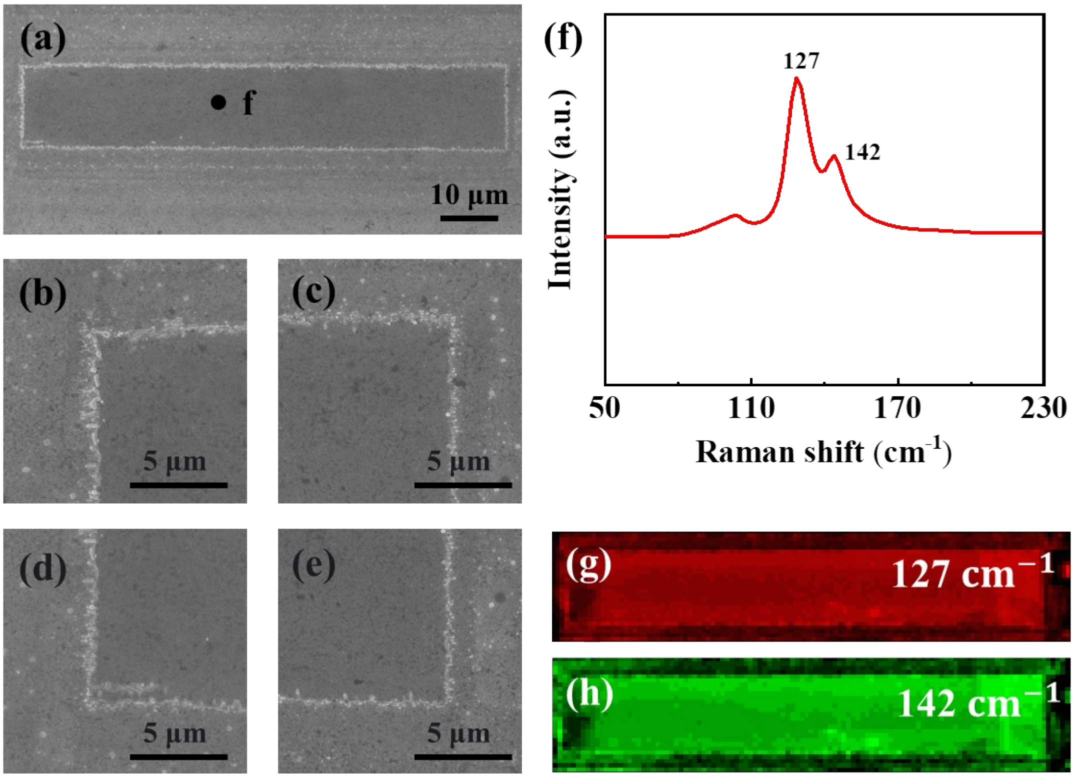

Fig. S16 (a) SEM image of an ultrafast laser tailored rectangular gallium telluride nanoflake on gold coated silicon wafer. (b-e) Magnified SEM images of ultrafast laser ablated corners in (a). (f) Raman spectra measured at the interior area indicated in (a). Raman mapping of rectangular gallium telluride nanoflake. The intensity represents for the characteristic peaks at (f) 127 cm^{-1} and (g) 142 cm^{-1}. Laser fluence: 1.56 J cm^{-2}. Pulse duration: 350 fs. Scanning speed: 10 μm/s. Repetition rate: 800 kHz.

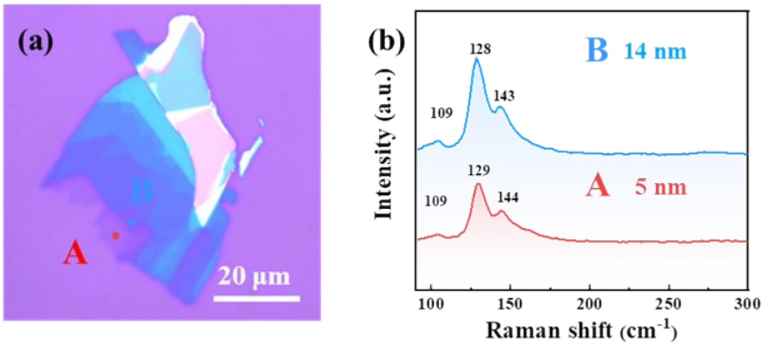

Fig. S17 (a) Optical image of pristine gallium telluride nanoflake on silica coated silicon wafer, and Point A and Point B in the figure correspond to the positions of relatively thinner and thicker sections, respectively. (b) Raman measurements of gallium telluride nanosheets at different positions.

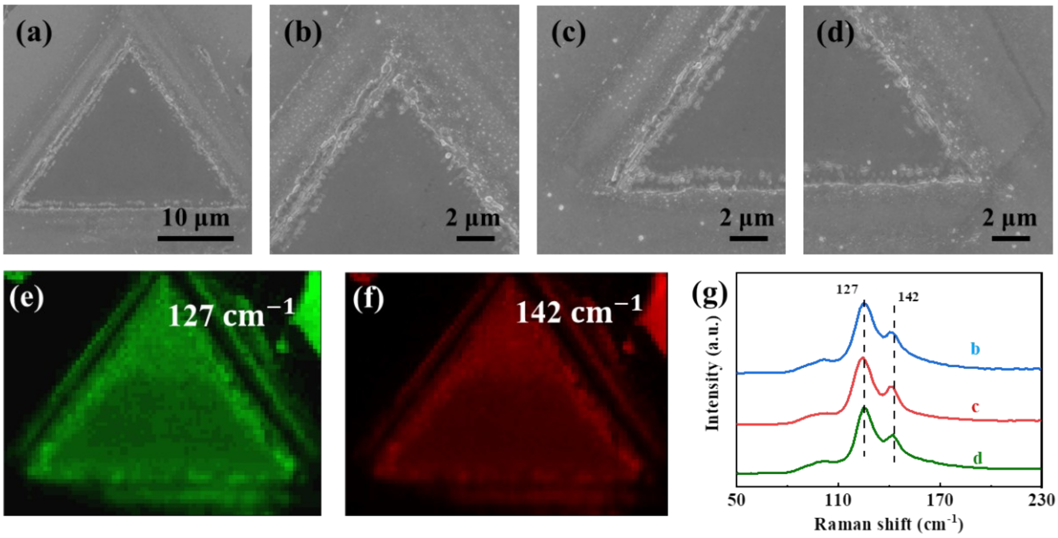

Fig. S18 (a) SEM image of an ultrafast laser tailored triangular gallium telluride nanoflake on gold coated silicon wafer. (b-d) Magnified SEM images of ultrafast laser ablated corners in (a). Scanning speed: 10 μm/s. Raman mapping of rectangular gallium telluride nanoflake. The intensity represents for the characteristic peaks at (e) 127 cm^{-1} and (f) 142 cm^{-1}. (g) Raman spectra measured at each angle of the triangle. Laser fluence: 1.56 J cm^{-2}. Pulse duration: 350 fs. Scanning speed: 10 μm/s. Repetition rate: 800 kHz.